HHS Public Access

Author manuscript

Exp Gerontol. Author manuscript; available in PMC 2021 May 01.

Published in final edited form as:

Exp Gerontol. 2020 May ; 133: 110872. doi:10.1016/j.exger.2020.110872.

Effects of *Gsta4* Deficiency on Age-related Cochlear Pathology and Hearing Loss in Mice

Hyo-Jin Park[a], **Mi-Jung Kim**[a], **Chul Han**[a], **Karessa White**[a], **Dalian Ding**[b], **Kevin Boyd**[a], **Richard Salvi**[b], **Shinichi Someya**[a,*]

[a]Department of Aging and Geriatric Research, University of Florida, Gainesville, FL 32611, USA

[b]Center for Hearing and Deafness, State University of New York at Buffalo, NY

Abstract

The glutathione transferase (GST) detoxification system converts exogenous and endogenous toxins into a less toxic form by conjugating the toxic compound to reduced glutathione (GSH) by a variety of GST enzymes. Of the ~20 GST isoforms, GSTA4 exhibits high catalytic efficiency toward 4-hydroxynonenal (4-HNE), one of the most abundant end products of lipid peroxidation that contributes to neurodegenerative diseases and age-related disorders. Conjugation to GSH by GSTA4 is thought to be a major route of 4-HNE elimination. In the current study, we investigated the effects of *Gsta4* deficiency on age-related cochlear pathology and hearing loss using young (3–5 months old) and old (24–25 months old) *Gsta4*$^{+/+}$ and *Gsta4*$^{-/-}$ mice that were backcrossed onto the CBA/CaJ mouse strain, a well-established model of age-related hearing loss (AHL). At 3–5 months of age, loss of *Gsta4* resulted in decreased total GSTA activity toward 4-HNE in the inner ears of young mice. However, there were no differences in the levels of 4-HNE in the inner ears between *Gsta4*$^{+/+}$ and *Gsta4*$^{-/-}$ mice at 3–5 or 24–25 months of age. No histological abnormalities were observed in the cochlea and no hearing impairments were observed in young *Gsta4*$^{-/-}$ mice. At 24–25 months of age, both *Gsta4*$^{+/+}$ and *Gsta4*$^{-/-}$ mice showed elevated ABR thresholds compared to 3-month-old mice, but there were no differences in ABR thresholds, cochlear spiral ganglion neuron densities, or stria vascularis thickness between *Gsta4*$^{+/+}$ and *Gsta4*$^{-/-}$ mice. Together, these results suggest that under normal physiological conditions or during normal aging, GSTA4 is not essential for removal of 4-HNE in mouse inner ears.

*Corresponding author: Department of Aging and Geriatric Research, University of Florida, Gainesville, Florida 32610, USA. Tel: 352-294-5167; fax: 352-294-5058; someya@ufl.edu.

Author contributions

Hyo-Jin Park: investigation, formal analysis, validation, writing - original draft **Mi-Jung Kim:** investigation, formal analysis **Chul Han:** investigation, formal analysis **Karessa White:** investigation, formal analysis **Dalian Ding:** investigation **Kevin Boyd:** investigation **Richard Salvi:** formal analysis, supervision, writing - review & editing **Shinichi Someya:** conceptualization, resources, writing - review & editing, supervision, project administration, funding acquisition

Conflict of interest

The authors declare that there are no conflicts of interest.

Keywords

glutathione transferase; detoxification; GSTA4; oxidative stress; age-related hearing loss

1. Introduction

Glutathione transferases (GSTs) are phase II detoxification enzymes that protect cellular macromolecules against naturally occurring toxins and foreign chemicals (Ayyadevara et al., 2007; Nebert and Vasiliou, 2004; Park et al., 2019; Sheehan et al., 2001). GSTs catalyze conjugation reactions of toxic compounds to reduced glutathione (GSH), producing a hydrophilic product that can be excreted from the cell through transmembrane transporters (Ayyadevara et al., 2007; McElwee et al., 2007; Nebert and Vasiliou, 2004; Park et al., 2019; Sheehan et al., 2001). GSTs are dimeric enzymes and widely distributed from bacteria to animals. Because of the diversity of potential xenobiotics and stressors, GSTs display extensive functional diversification in gene expression, enzyme activities, and substrate specificities. The most well characterized cytosolic GST classes have been named alpha (GSTA), mu (GSTM), pi (GSTP), and theta (GSTT). Because of their cytoprotective role and involvement in the development of resistance to anti-cancer agents, GSTs have become attractive drug targets (Nebert and Vasiliou, 2004; Sheehan et al., 2001).

Of the ~20 mammalian GSTs that have been identified to date, GSTA4 possesses high catalytic efficiency toward cytotoxic lipid-derived aldehydes, including 4-hydroxynonenal (4-HNE), one of the most abundant end products of lipid peroxidation that contributes to neurodegenerative diseases, aging, and cancer (Bared et al., 2010; Chen et al., 2014; Han et al., 2016; Rahman et al., 2007; Van Eyken et al., 2007). Conjugation to GSH by GSTA4 is thought to be a major route of 4-HNE elimination. Previous studies have shown that knockdown of either *gst-5* or *gst-10* with high catalytic activity toward 4-HNE, shortens life span, while overexpression of *gst-10* or murine *Gsta4* extends lifespan in *C. elegans* (Ayyadevara et al., 2007, 2005). A cross-species comparative analysis has also shown that GST and other cellular detoxification gene categories were significantly up-regulated in long-lived *C. elegans* (*daf-2*), *D. melanogaster* (*chico*$^{1/+}$), Ames dwarf mice (*Prop1*$^{df/df}$), and Little dwarf mice (*Ghrhr*$^{lit/lit}$) (McElwee et al., 2007), suggesting that cellular detoxification might play a broader role in longevity or protection against aging in multiple species. Consistent with those reports, Ames dwarf mice (*Prop1*$^{df/df}$), which show a 50% increase in lifespan, display increased levels of liver glutamate-cysteine ligase, the rate-limiting enzyme in the glutathione biosynthesis pathway, and increased total GST activity in the kidneys at 3 and 24 months of age (Brown-Borg and Rakoczy, 2005). In humans, *GSTM1*, *GSTP1*, and *GSTT1* polymorphisms were detected in noise-exposed workers in Taiwan (Lin et al., 2009), while a significant association between AHL and *GSTT1* and *GSTM1* polymorphisms was found in a Finnish population (Van Eyken et al., 2007) and Hispanic population (Bared et al., 2010). Together, these results suggest that GSTA4 detoxification or GSTA4-mediated detoxification of 4-HNE might play an important role in slowing age-related disorders.

Hearing loss is the third most prevalent chronic health condition affecting older adults and AHL, also known as presbycusis, is the most common form of hearing impairment (Gates

and Mills, 2005; Ozmeral et al., 2016; Yamasoba et al., 2013). AHL is characterized by poor speech understanding particularly in noise, impaired temporal resolution, and central auditory processing deficits (Gates and Mills, 2005; Ozmeral et al., 2016; Yamasoba et al., 2013). WHO estimates that one-third of persons over 65 years are affected by disabling hearing loss (2019). Worldwide, approximately 466 million people suffer from hearing impairment and this number is expected to rise to 630 million by 2030 and over 900 million in 2050 (WHO 2010). Because the prevalence of AHL is expected to rise dramatically as the world's population ages, AHL will become a major social and health care problem.

In the current study, we investigated the effects of *Gsta4* deficiency on age-related cochlear pathology and hearing loss using young (3–5 months old) and old (24–25 months old) *Gsta4*$^{+/+}$ and *Gsta4*$^{-/-}$ mice that were backcrossed onto the CBA/CaJ mouse strain, a well-established model of AHL (Ahmed et al., 2010; Park et al., 2019; Voghel et al., 2008; Zimniak et al., 1994). At 3–5 months of age, loss of *Gsta4* resulted in decreased total GSTA activity toward 4-HNE in the inner ears of young mice. However, there were no differences in the levels of 4-HNE in the inner ears between *Gsta4*$^{+/+}$ and *Gsta4*$^{-/-}$ mice at 3–5 or 24–25 months of age. No histological abnormalities were observed in the cochlea and no hearing impairments were observed in young *Gsta4*$^{-/-}$ mice. At 24–25 months of age, both *Gsta4*$^{+/+}$ and *Gsta4*$^{-/-}$ mice showed elevated ABR thresholds compared to 3-month-old mice, but there were no differences in ABR thresholds or cochlear spiral ganglion neuron densities between *Gsta4*$^{+/+}$ and *Gsta4*$^{-/-}$ mice. Together, these results suggest that under normal physiological conditions or during normal aging, GSTA4 is not essential for removal of 4-HNE in mouse inner ears.

2. Materials and Methods

2.1. Animals

Male and female *Gsta4*$^{+/-}$ mice were obtained from the Mutant Mouse Regional Resource Centers (MMRRC) (https://www.mmrrc.org/catalog/sds.php?mmrrc_id=11713) at Lexicon Genetics. The *Gsta4* knockout allele was generated by inserting a gene trap cassette (5174 nucleotides) into intron 1 and it is expected to be completely null in GSTA4 expression. Male and female CBA/CaJ mice were obtained from Jackson Laboratory (https://www.jax.org/strain/000654). All animal studies were conducted at the AAALAC-approved University of Florida Animal Facility. Experiments were performed in accordance with protocols approved by the University of Florida Institutional Animal Care and Use Committee. *Gsta4*$^{+/-}$ heterozygous males were mated with *Gsta4*$^{+/-}$ heterozygous females and their offspring were genotyped with DNA extracted from a tail clip obtained at weaning as previously described (Park et al., 2019). Male and female *Gsta4*-deficient mice have been backcrossed for 6 generations onto the CBA/CaJ mouse strain that does not carry the recessive AHL-susceptibility allele (*Cdh23*^{753A}). To confirm that *Gsta4*$^{+/+}$ and *Gsta4*$^{-/-}$ mice have the same wild-type *Cdh23*$^{753G/753G}$ genotype for *Cdh23*, we isolated DNA from these animals, amplified by PCR and then sequenced the region of DNA containing the 753rd nucleotide in the *Cdh23* gene as previously described (Park et al., 2019). Both male and female *Gsta4*$^{+/+}$ and *Gsta4*$^{-/-}$ littermates were used in the current study.

2.2. Assessment of ABR

Auditory brainstem responses (ABRs) were measured with a tone burst stimulus at 4, 8, 16, 32, 48 and 64 kHz using the TDT neurophysiology workstation (Tucker-Davis Technologies) in a sound isolation booth as previously described (Han et al., 2016). Briefly, mice were anesthetized with a mixture of xylazine (10 mg/kg) and ketamine (100 mg/kg) by intraperitoneal injection and placed on a warm heating pad. Needle electrodes were placed subcutaneously at the vertex (non-inverting or active), ipsilateral ear (reference), and contralateral ear (ground). At each frequency, the sound level was decreased in 5–10 dB SPL steps from 90 to 10 dB sound pressure level (SPL). A hearing threshold was defined as the lowest level that produced a noticeable ABR. ABR amplitudes and latencies for wave I were measured at 8, 16, 32, and 48 kHz at 90 dB SPL for all animals. A wave I amplitude was determined by measuring the voltage difference between the highest positive value (peak) and greatest negative value (trough) for the first ABR wave as previously described by Chen et al. (Chen et al., 2014). A wave I latency was measured as the amount of time elapsed from the onset of the stimulus to the peak of the first wave. We used 6–8 mice per group for ABR threshold, amplitude, and latency assessments. Following the ABR hearing measurements, tissues from the same mice were used to conduct histological, biochemical, or molecular analyses.

2.3. GST activity

Labyrinth tissues including bony shell, cochlear lateral wall, cochlear basilar membrane, cochlear modiolus, utricle, saccule, and three semicircular canals were homogenized using a tissue grinder (Wheaton Dounce Tissue Grinder, Fisher Scientific) containing 1 ml of Tris buffer (10 mM Tris, 1 mM EDTA, 320 mM sucrose, pH 7.4) on ice and then centrifuged at 10,000 g for 10 min at 4 °C. The supernatant (cytosolic fraction) was used for GST analyses. For GST activity toward 4-hydroxynonenal (4-HNE), 10 μl of cytosolic lysate was added to a well in the 96 well plate and then 190 μl of mixture containing 5 mM L-Glutathione reduced and 2 mM 4-HNE in 100 mM potassium phosphate buffer (pH 6.5) added to the well. The absorbance was read at 225 nm every 30 s for 10 min in a spectrophotometer (Bio-Tek) to calculate activity. The GST activity was normalized to total protein. All samples were run in duplicate. GST activity toward 1-chloro-2,4- dinitrobenzene (CDNB) was measured using the GST Assay kit (Sigma-Aldrich) according to the manufacturer's instructions. In brief, 20 μl of cytosolic lysate was added to a well in the 96 well plate and then 180 μl of mixture containing 176.4 μl of Dulbecco's phosphate buffered saline (DPBS), 1.8 μl of 200 mM L-Glutathione reduced, and 1.8 μl of 100 mM CDNB was added to the well. The absorbance was read at 340 nm every minute for 6 min in a spectrometer (Bio-Tek) to calculate the activity. All samples were run in duplicate.

2.4. Glutathione redox state

Labyrinth tissues were homogenized using a tissue grinder (Wheaton Dounce Tissue Grinder, Fisher Scientific) containing 1 ml of lysis buffer (10 mM Tris, 20 mM EDTA, 320 mM sucrose, pH 7.4) on ice and then centrifuged at 10,000 g for 10 min at 4 °C to obtain a cytosolic lysate (supernatant). One hundred microliter of the cytosolic lysate was used for the measurements of GSH, GSSG, and GSH/GSSG levels. Total glutathione (GSH + GSSG)

and GSSG levels were determined by the method of Rahman et al. (Rahman et al., 2007). Briefly, the rates of 5'-thio-2-nitrobenzoic acid (TNB) formation were calculated, and the total glutathione (tGSH) and GSSG concentrations in the samples were determined by using linear regression to calculate the values obtained from the standard curve. The GSH concentration was determined by subtracting the GSSG concentration from the total glutathione concentration. All samples were run in duplicate. All reagents used in this assay were purchased from Sigma-Aldrich unless indicated otherwise.

2.5. Protein carbonyl

Labyrinth tissues were homogenized using a tissue grinder (Wheaton Dounce Tissue Grinder, Fisher Scientific) containing 1 ml of Tris buffer (10 mM Tris, 1 mM EDTA, 320 mM sucrose, pH 7.4) on ice and then centrifuged at 15,000 × g for 10 min at 4 °C. Levels of the oxidative protein damage marker, protein carbonyl, were measured with inner ear whole cell lysate using the Oxyblot Protein Oxidation Detection kit (EMD Millipore) according to the manufacturer's instructions. In brief, 8 μg of lysates were denatured by adding the same volume of 12% SDS for a final concentration of 6% SDS and were derivatized by adding 2 volumes of 1x DNPH solution to the tube and incubated at room temperature for 15 min. One and a half volumes of neutralization solution were added to the tube to stop the reaction. 2-mercaptoethanol (1–1.5μL; 5% v/v) was added to the tube to achieve a final concentration of 0.74 M solution. Samples were loaded into a polyacrylamide gel (4–20%) (Bio-Rad) and separated at 100 V for 90 min. Proteins on the gel were transferred to a nitrocellulose membrane (Bio-Rad). The membrane was incubated with blocking buffer (4 % skim milk in PBS) for 1 h. The membrane was incubated with the primary antibody (1:150, diluted in the blocking buffer) overnight at 4 °C. The membrane was washed with PBS-T containing 0.05 % (v/v) tween-20 (Sigma-Aldrich) in PBS for 10 min three times. The membrane was incubated with the secondary antibody (1:300, diluted in the blocking buffer) for 1 h at room temperature. The membrane was washed with PBS-T for 10 min three times. The membrane was developed with Amersham ECL Prime (GE healthcare). The intensity of bands was quantified using ImageJ software (National Institutes of Health).

2.6. Assessment of Cochlear Pathology

2.6.1. Cochlear tissue preparation—Following the ABR measurements, the animals were sacrificed by cervical dislocation and the temporal bones were excised from the head as previously described (Someya et al., 2010). The temporal bones were immersed in a fixative containing 4% paraformaldehyde (Sigma-Aldrich) in phosphate buffered saline (PBS) solution for 1 d, decalcified in 10% EDTA for 1 week, divided into cochlear and vestibular parts, and then embedded in paraffin. The paraffin-embedded specimens were sliced along the mid-modiolar axis into 5 μm sections, mounted on silane-coated slides, stained with H&E, and observed under a light microscope (Leica). Rosenthal's canal was divided into three regions: apical, middle and basal and the three regions were used for evaluation of cochlear pathology. Tissues from the same animals were used for cochleograms, spiral ganglion neuron (SGN) counting, and stria vascularis thickness measurements.

2.6.2. Cochleogram—The number of inner hair cells (IHCs) and outer hair cells (OHCs) were counted over 0.24 mm intervals along the entire length of the cochlea under the microscope at 400× magnification as previously described (Ding et al., 2013, 1999). The counting results were then entered into a custom computer program designed to compute a cochleogram that shows the number of missing IHCs and OHCs as a function of percentage distance from the apex of the cochlea. The frequency-place map for mouse cochlea was shown on the abscissa in the figures as previously described (Ding et al., 2016; Müller et al., 2005).

2.6.3. SGN Density—SGN densities were measured in the apical, middle, and basal regions of the cochlear sections using a 40x objective as previously described (Someya et al., 2010). Type I and type II neurons were not differentiated. Cells were identified by the presence of a nucleus. The corresponding area of the Rosenthal canal was measured in digital photomicrographs of each canal profile. The perimeter of the canal was traced with a cursor using ImageJ software (National Institutes of Health). The software then calculated the area within the outline. The SGN density was calculated as the number of SGNs per mm^2. Four to twenty sections of the apical, middle, and basal turns were evaluated in one cochlea per mouse. We used 3–5 mice per group for assessment of SGN density.

2.6.4. SV thickness—SV thickness was measured in 40X images of H&E-stained mouse cochlear tissues. Stria vascularis thickness was measured by using a cursor to draw a line from the margin of the stria to the junction of the basal cells with the spiral ligament halfway between the attachment of Reissner's membrane and the spiral prominence using the ImageJ software (National Institutes of Health) (Han et al., 2016). Measurements were made at the basal, middle and apical regions of the cochlea for each mouse. Five to twenty sections of the apical, middle and basal turns were evaluated in one cochlea per mouse. We used 3–5 mice per group for stria vascularis thickness measurements.

2.7. Statistical analysis

Two-way ANOVA with Bonferroni's *post hoc* test (GraphPad Prism 4.03) was used to analyse ABR threshold, SGN density, SV thickness, and hair cell loss. Student t-tests (GraphPad Prism 4.03) was used to analyse GST activities and levels of GSH and GSSG and protein carbonyl.

3. Results

3.1. Gsta4 deficiency does not affect auditory function in young mice

To investigate the effects of *Gsta4* deficiency on age-related cochlear pathology and hearing loss, $Gsta4^{+/-}$ mice were backcrossed for 6 generations onto the CBA/CaJ mouse strain, a normal-hearing strain that does not carry the recessive early-onset hearing loss-susceptibility allele ($Cdh23^{753A}$) (Noben-Trauth et al., 2003; Zheng et al., 1999). We confirmed the absence of *Gsta4* by PCR genotyping and then sequenced the *Cdh23* gene in the DNA obtained from tails of young $Gsta4^{+/+}$ and $Gsta4^{-/-}$ mice. We confirmed that all $Gsta4^{+/+}$ and $Gsta4^{-/-}$ mice had the same wild-type genotype ($Cdh23^{753G/753G}$) as previously

described (Park et al., 2019). Mice lacking the *Gsta4* gene on the CBA/CaJ background appeared phenotypically normal, are viable and fertile (Park et al., 2019).

To investigate the effects of *Gsta4* deficiency on auditory function, we first measured ABR (auditory brainstem response) thresholds with a tone burst stimulus over a broad frequency range (4–64 kHz) in male and female *Gsta4*$^{+/+}$ and *Gsta4*$^{-/-}$ mice at 3–5 months. There were no differences in ABR thresholds at 4, 8, 16, 32, 48 or 64 kHz between male (Fig. 1A) or female (Fig. 1B) *Gsta4*$^{+/+}$ and *Gsta4*$^{-/-}$ mice (Fig. 1A–B). In rodents, ABRs typically consist of 5 positive waves; waves I-II represent activity from the auditory nerve, while waves III-V represent neural transmission within the central auditory system (Zhou et al., 2006). To further assess hearing sensitivity and the functional integrity of the auditory nerve, ABR latencies and amplitudes for wave I were measured at 8, 16, 32, and 48 kHz at 90 dB SPL in male and female WT and *Gsta4*$^{-/-}$ mice at 3–5 months of age. Consistent with the ABR threshold results, there were no differences in ABR wave I amplitudes (Fig. 1C–D) or latencies (Fig. 1E–F) at 8, 16, 32 or 48 kHz between male or female *Gsta4*$^{+/+}$ and *Gsta4*$^{-/-}$ mice. Together, these results indicate that *Gsta4* deficiency does not affect auditory function in young mice.

3.2. Gsta4 deficiency decreases GST activity, but does not increase 4-HNE, GSSG, or protein carbonyl levels in the inner ears of young mice

GSTA4 has high-catalytic efficiency toward 4-HNE, a cytotoxic end product of lipid peroxidation that covalently modifies protein and DNA (Bared et al., 2010; Park et al., 2019; Rahman et al., 2007; Van Eyken et al., 2007). Hence, we hypothesized that *Gsta4* deficiency may result in elevated levels of 4-HNE in inner ear tissues from young mice. To test this hypothesis, we first measured GST activities using 4-HNE as a specific substrate for GSTA4 and CDNB, a general substrate for most GSTs, in inner ear tissues from 3–5 months old *Gsta4*$^{+/+}$ and *Gsta4*$^{-/-}$ mice. Because there were no gender differences in ABR thresholds, wave I amplitudes or latencies at all the frequencies measured between young *Gsta4*$^{+/+}$ and *Gsta4*$^{-/-}$ mice, subsequent tissues analysis was conducted in male mice. As expected, young *Gsta4*$^{-/-}$ mice displayed a 75% decrease in GSTA4 activities toward 4-HNE in the inner ears compared to *Gsta4*$^{+/+}$ mice (Fig. 2A). But, there was no difference in GST activities toward CDNB between *Gsta4*$^{+/+}$ and *Gsta4*$^{-/-}$ mice (Fig. 2B). Next, to investigate whether *Gsta4* deficiency results in elevated levels of inner ear 4-HNE, we counted 4-HNE-positive SGNs in cochlear sections from 3–5 months old male *Gsta4*$^{+/+}$ and *Gsta4*$^{-/-}$ mice. There were no differences in 4-HNE levels in the apical, middle, or basal cochlear regions between *Gsta4*$^{+/+}$ and *Gsta4*$^{-/-}$ mice (Fig. 2C).

GSTs convert exogenous and endogenous toxins into a less toxic form by conjugating the toxic compound to GSH by a variety of GST enzymes (Henderson and Wolf, 2011; Laborde, 2010). Thus, GSH plays a critical role in Phase II cellular detoxification by serving as a substrate for GSTs in detoxifying toxins. To investigate the effects of *Gsta4* deficiency on glutathione redox state, we measured the levels of oxidized glutathione (GSSG), reduced glutathione (GSH), and total glutathione in the cytosol of the inner ear tissues from 3–5 months old male *Gsta4*$^{+/+}$ and *Gsta4*$^{-/-}$ mice. There were no differences in GSH, GSSG or GSH/GSSG in the inner ears between *Gsta4*$^{+/+}$ and *Gsta4*$^{-/-}$ mice (Fig. 3A). We also

measured levels of protein carbonyl, a marker of oxidative protein damage, in the inner ears from 3–5 months old male *Gsta4*$^{+/+}$ and *Gsta4*$^{-/-}$ mice. There were no differences in the levels of protein carbonyl in the inner ears between *Gsta4*$^{+/+}$ and *Gsta4*$^{-/-}$ mice (Fig. 3B). Together, these results indicate that *Gsta4* deficiency results in decreased GST activity toward 4-HNE in the inner ears of young mice; however, *Gsta4* deficiency does not result in accumulation of 4-HNE in the inner ears of young mice.

3.3. Gsta4 deficiency does not promote AHL in mice

To investigate the effects of *Gsta4* deficiency on auditory function in older mice, we measured ABR thresholds with a tone burst stimulus over a broad frequency range (4–64 kHz) in *Gsta4*$^{+/+}$ and *Gsta4*$^{-/-}$ mice at 24–25 months. Because there were no gender differences in ABR thresholds, wave I amplitudes or latencies at all the frequencies measured between young *Gsta4*$^{+/+}$ and *Gsta4*$^{-/-}$ mice, subsequent ABR and pathological analyses were conducted in males. As expected, both old *Gsta4*$^{+/+}$ and *Gsta4*$^{-/-}$ mice showed elevated ABR thresholds at 4–64 kHz compared to young mice (Fig. 4A–B). However, there were no differences in ABR thresholds at all the frequencies measured between old *Gsta4*$^{+/+}$ and *Gsta4*$^{-/-}$ mice (Fig. 4C). To further assess hearing sensitivity and the functional integrity of the auditory nerve in old *Gsta4*$^{+/+}$ and *Gsta4*$^{-/-}$ mice, we measured ABR amplitudes and latencies for wave I at 8, 16, 32, and 48 kHz at 90 dB SPL at 24–25 months. Both old *Gsta4*$^{+/+}$ and *Gsta4*$^{-/-}$ mice showed decreased ABR wave I amplitudes at 8–48 kHz compared to young mice (Fig. 5A–D), but there were no differences in ABR wave I amplitudes or latencies at all the frequencies measured between old *Gsta4*$^{+/+}$ and *Gsta4*$^{-/-}$ mice (Fig. 5A–H).

The major sites of cochlear pathology typically include cochlear hair cells, SGN and stria vascularis (Gates and Mills, 2005; Yamasoba et al., 2013). To validate the ABR test results and to investigate the effects of *Gsta4* deficiency on age-related cochlear pathology, mean cochleograms were prepared from 3–5 month-old and 24–25 month-old male *Gsta4*$^{+/+}$ and *Gsta4*$^{-/-}$ mice. At 3–5 months of age, no loss of inner hair cells (IHCs) (Fig. 6A) or outer hair cells (OHCs) (Fig. 6B) were observed in the cochleae from *Gsta4*$^{+/+}$ and *Gsta4*$^{-/-}$ mice. At 24–25 months of age, little or no loss of IHCs was observed in the apical or middle cochlea regions from both *Gsta4*$^{+/+}$ and *Gsta4*$^{-/-}$ mice. In the basal region, *Gsta4*$^{-/-}$ mice showed a slight but significantly greater loss of IHCs compared to age-matched *Gsta4*$^{+/+}$ mice (Fig. 6C). Little or no loss of OHCs was observed in the middle or basal cochlea regions from both *Gsta4*$^{+/+}$ and *Gsta4*$^{-/-}$ mice. In the apical region, *Gsta4*$^{-/-}$ mice showed a slight but significantly greater loss of OHCs compared to age-matched *Gsta4*$^{+/+}$ mice (Fig. 6D).

Next, we measured the densities of SGNs in the apical, middle, and basal regions of the cochleae from 3–5 month-old and 24–25 month-old male *Gsta4*$^{+/+}$ and *Gsta4*$^{-/-}$ mice. At 3–5 months of age, there were no differences in SGN densities in the cochleae between *Gsta4*$^{+/+}$ and *Gsta4*$^{-/-}$ mice (Fig. 7A–F, M-O). At 24–25 months of age, there were no differences in SGN densities in the apical, middle, or basal regions between *Gsta4*$^{+/+}$ and *Gsta4*$^{-/-}$ mice (Fig. 7G–O). Atrophy of the stria vascularis is one of the most prominent features of AHL (Gates and Mills, 2005; Shuknecht et al., 1974; Yamasoba et al., 2013). To

investigate the effects of *Gsta4* deficiency on age-related stria vascularis (SV) atrophy, we measured the SV thickness in the apical, middle, and basal regions of the cochlea from 3–5 month-old and 24–25 month-old male *Gsta4*$^{+/+}$ and *Gsta4*$^{-/-}$ mice. At 3–5 months of age, there were no differences in SV thickness in the cochlea between *Gsta4*$^{+/+}$ and *Gsta4*$^{-/-}$ mice (Fig. 8A–F, M–O). At 24–25 months of age, there were no differences in SV thickness in the apical, middle, or basal regions between *Gsta4*$^{+/+}$ and *Gsta4*$^{-/-}$ mice (Fig. 8G–O).

Lastly, to investigate whether *Gsta4* deficiency results in elevated levels of 4-HNE in aged cochlear tissues, we measured 4-HNE levels in the apical, middle, and basal regions of the cochleae from 3–5 month-old and 24–25 month-old male *Gsta4*$^{+/+}$ and *Gsta4*$^{-/-}$ mice. As expected, both *Gsta4*$^{+/+}$ and *Gsta4*$^{-/-}$ mice showed elevated levels of 4-HNE in the apical and middle regions of the cochleae (Fig. 2E–F), but there were no differences in 4-HNE levels in any cochlear regions between old *Gsta4*$^{+/+}$ and *Gsta4*$^{-/-}$ mice (Fig. 2D). Taken together, these physiological and histological results indicate that during normal aging, *Gsta4* deficiency does not result in increased levels of 4-HNR, more profound loss of SGNs or more profound hearing impairments in mice.

4. Discussion

A growing body of evidence indicates that ROS play a major role in the age-related degeneration of cochlear hair cells and SGNs during aging (Cheng et al., 2005; Someya et al., 2009; Yamasoba et al., 2013). At the membrane levels, ROS cause the oxidation of polyunsaturated fatty acids, leading to the formation of cytotoxic aldehydes, including 4-HNE, one of the most abundant end product of lipid peroxidation that covalently modifies protein and DNA (Ayyadevara et al., 2005; Board, 1998; Di Domenico et al., 2017; Engle et al., 2004; Zimniak et al., 1994). The central nervous system and the peripheral nervous system are particularly sensitive to ROS damage because of the high levels of polyunsaturated fatty acids in neuronal cell membranes (Di Domenico et al., 2017). Accordingly, elevated levels of 4-HNE have been observed in brain tissues of Alzheimer disease, Parkinson disease, and Huntington disease patients and animal models of these neurodegenerative diseases. GSTA4 is thought to be a major detoxification enzyme which removes 4-HNE by catalysing the conjugation reaction of 4-HNE to GSH (Ayyadevara et al., 2005; Board, 1998; Engle et al., 2004; Zimniak et al., 1994). This idea is supported by previous reports that GST activity toward 4-HNE is significantly reduced in the kidney, lung, heart, brain, muscle, spleen, and intestine of *Gsta4* KO mice (Engle et al., 2004) and that 4-HNE-adducts accumulate with aging *in vivo* and *in vitro* (Ahmed et al., 2010; Voghel et al., 2008). Moreover, accumulation of 4-HNE is linked to age-related diseases associated with increased levels of oxidative stress or redox imbalance, including Alzheimer's disease (Rockwell et al., 2000; Shringarpure et al., 2000), Parkinson disease (Ebara et al., 2003; Jenner, 2003), cancer (Feng et al., 2004), atherosclerosis (Herbst et al., 1999), and liver diseases (Singh et al., 2009). 4-HNE is also considered as an apoptosis inducer *in vitro* and *in vivo* (Dalleau et al., 2013). In *C. elegans*, loss of *gst-10* that encodes a detoxifying enzyme with high catalytic activity toward 4-HNE results in reduced lifespan (Ayyadevara et al., 2007). In the current study, we demonstrated that loss of *Gsta4* resulted in a significant decline in GST activity toward 4-HNE in the inner ears of young mice. However, although both 24-month-old *Gsta4*$^{+/+}$ and *Gsta4*$^{-/-}$ mice showed elevated levels of 4-HNE compared

to young mice, there were no differences in 4-HNE levels in the cochlea between old *Gsta4*$^{+/+}$ and *Gsta4*$^{-/-}$ mice (Fig. 2). Both *Gsta4*$^{+/+}$ and *Gsta4*$^{-/-}$ mice also showed elevated ABR thresholds and wave I amplitudes at 24–25 months of age (Fig. 5A–D), but there were no differences in ABR thresholds or ABR wave I amplitudes between old *Gsta4*$^{+/+}$ and *Gsta4*$^{-/-}$ mice (Fig. 5A–H). In agreement with the physiological results, there were no differences in SGN densities (Fig. 7) or SV thickness (Fig. 8) in the cochleae between aged *Gsta4*$^{+/+}$ and *Gsta4*$^{-/-}$ mice. Old *Gsta4*$^{-/-}$ mice showed slightly greater loss of OHCs in the apical region, but in general, there were no major differences in IHC or OHC loss in the cochleae between aged *Gsta4*$^{+/+}$ and *Gsta4*$^{-/-}$ mice (Fig. 6). Together, these previous reports and our findings suggest that during normal aging, GSTA4 is not essential for removal of 4-HNE in mouse inner ears or that *Gsta4* deficiency is not sufficient to promote age-related cochlear pathology or hearing loss in mice.

Shearn et al. have shown that chronic consumption of ethanol resulted in increased levels of HNE-protein adducts in the liver of *Gsta4* KO mice (Shearn et al., 2016), while chronic treatment of the herbicide paraquat significantly shortened the survival of *Gsta4* KO mice compared to wild-type mice (Zimniak et al., 1994). Dwivedi et al have also shown that administration of hepatotoxic carbon tetrachloride resulted in significantly higher levels of 4-HNE in the liver of *Gsta4*$^{-/-}$ mice compared to *Gsta4*$^{+/+}$ mice (Dwivedi et al., 2006). Our group has recently shown that administration of cisplatin, an ototoxic chemotherapeutic drug, resulted in more profound hearing loss, and more profound loss of SGNs, and atrophy of SV in female *Gsta4*$^{-/-}$ mice (Park et al., 2019). Cisplatin treatment also resulted in increased levels of 4-HNE in the cochlea of female *Gsta4*$^{-/-}$ mice compared to age-matched *Gsta4*$^{+/+}$ mice (Park et al., 2019). In the current study, aging did not result in higher levels of inner ear 4-HNE, more profound loss of SGNs, or hearing loss in *Gsta4*$^{-/-}$ mice when compared to age-matched *Gsta4*$^{+/+}$ mice. Therefore, under treatment with ototoxic drugs/chemicals or higher levels of 4-HNE, loss of *Gsta4* likely leads to more profound loss of cochlear neurons and hair cells and accelerated hearing loss.

Cells possess a wide range of mechanisms for detoxifying 4-HNE: Reduced glutathione (GSH) can sequester 4-HNE by forming GSH-HNE adducts, while carnosine can sequester 4-HNE via intramolecular Michael addition (Di Domenico et al., 2017). 4-HNE can also be detoxified by aldo-keto reductase, aldose reductase, and aldehyde dehydrogenase (Srivastava et al., 1995; Black et al., 2012). Furthermore, GSTA1, GSTA2, GSTM1, and GSTT1 also possess antioxidant activity toward lipid hydroperoxides, including 4-HNE (Ayyadevara et al., 2007; Brown-Borg and Rakoczy, 2005; Han et al., 2016; Park et al., 2019; Sheehan et al., 2001). Therefore, under normal physiological conditions, low-moderate levels of 4-HNE, or during normal aging, one or some of these antioxidants and/or enzymes likely compensates for the loss of GSTA4 in removing 4-HNE in inner ears.

Acknowledgements

This research was supported by R03 DC011840 (SS), R01 DC012552 (SS) and R01 DC014437 (SS) from the National Institute of Health and National Institute on Deafness and Communication Disorders, and the Claude D. Pepper Older Americans Independence Centers at the University of Florida (P30 AG028740) from the National Institute of Health and National Institute on Aging.

References

https://www.mmrrc.org/catalog/sds.php?mmrrc_id=11713

https://www.jax.org/strain/000654

Ahmed EK, Rogowska-Wrzesinska A, Roepstorff P, Bulteau AL, Friguet B, 2010 Protein modification and replicative senescence of WI-38 human embryonic fibroblasts. Aging Cell 9, 252–272. [PubMed: 20102351]

Ayyadevara S, Dandapat A, Singh SP, Siegel ER, Shmookler Reis RJ, Zimniak L, Zimniak P, 2007 Life span and stress resistance of Caenorhabditis elegans are differentially affected by glutathione transferases metabolizing 4-hydroxynon-2-enal. Mech. Ageing Dev. 128, 196–205. [PubMed: 17157356]

Ayyadevara S, Engle MR, Singh SP, Dandapat A, Lichti CF, Beneš H, Shmookler Reis RJ, Liebau E, Zimniak P, 2005 Lifespan and stress resistance of Caenorhabditis elegans are increased by expression of glutathione transferases capable of metabolizing the lipid peroxidation product 4-hydroxynonenal. Aging Cell 4, 257–271. [PubMed: 16164425]

Bared A, Ouyang X, Angeli S, Du LL, Hoang K, Yan D, Liu XZ, 2010 Antioxidant enzymes, presbycusis, and ethnic variability. Otolaryngol. - Head Neck Surg. 143, 263–268.

Black W, Chen Y, Matsumoto A, Thompson DC, Lassen N, Pappa A, Vasiliou V, 2012 Molecular mechanisms of ALDH3A1-mediated cellular protection against 4-hydroxy-2-nonenal. Free Radic Biol Med. 52(9):1937–1944. [PubMed: 22406320]

Board PG, 1998 Identification of cDNAs encoding two human Alpha class glutathione transferases (GSTA3 and GSTA4) and the heterologous expression of GSTA4–4. Biochem. J 330, 827–831. [PubMed: 9480897]

Brown-Borg HM, Rakoczy SG, 2005 Glutathione metabolism in long-living Ames dwarf mice. Exp. Gerontol 40, 115–120. [PubMed: 15664737]

Chen G. Di, Decker B, Krishnan Muthaiah VP, Sheppard A, Salvi R, 2014 Prolonged noise exposure-induced auditory threshold shifts in rats. Hear. Res 317, 1–8. [PubMed: 25219503]

Cheng AG, Cunningham LL, Rubel EW, 2005 Mechanisms of hair cell death and protection. Curr. Opin. Otolaryngol. Head Neck Surg

Dalleau S, Baradat M, Guéraud F, Huc L, 2013 Cell death and diseases related to oxidative stress:4-hydroxynonenal (HNE) in the balance. Cell Death Differ. 20, 1615–1630. [PubMed: 24096871]

Di Domenico F, Tramutola A, Butterfield DA, 2017 Role of 4-hydroxy-2-nonenal (HNE) in the pathogenesis of alzheimer disease and other selected age-related neurodegenerative disorders. Free Radic. Biol. Med

Ding D, Jiang H, Chen G. Di, Longo-Guess C, Krishnan Muthaiah VP, Tian C, Sheppard A, Salvi R, Johnson KR, 2016 N-acetyl-cysteine prevents age-related hearing loss and the progressive loss of inner hair cells in γ-glutamyl transferase 1 deficient mice. Aging (Albany. NY). 8, 730–750. [PubMed: 26977590]

Ding D, Li M, Zheng X, Wang J, Salvi RJ, 1999 Cochleogram for assessing hair cells and efferent fibers in carboplatin-treated ear. Lin Chuang Er Bi Yan Hou Ke Za Zhi 13, 510–512. [PubMed: 12541378]

Ding D, Qi W, Yu D, Jiang H, Han C, Kim MJ, Katsuno K, Hsieh YH, Miyakawa T, Salvi R, Tanokura M, Someya S, 2013 Addition of exogenous NAD + prevents mefloquine-induced neuroaxonal and hair cell degeneration through reduction of caspase-3-mediated apoptosis in cochlear organotypic cultures. PLoS One 8, 1–12.

Dwivedi S, Sharma R, Sharma A, Zimniak P, Ceci JD, Awasthi YC, Boor PJ, 2006 The course of CCl4 induced hepatotoxicity is altered in mGSTA4–4 null (−/−) mice. Toxicology 218, 58–66. [PubMed: 16325313]

Ebara M, Fukuda H, Saisho H, 2003 The copper/zinc ratio in patients with hepatocellular carcinoma. J. Gastroenterol

Engle MR, Singh SP, Czernik PJ, Gaddy D, Montague DC, Ceci JD, Yang Y, Awasthi S, Awasthi YC, Zimniak P, 2004 Physiological role of mGSTA4–4, a glutathione S-transferase metabolizing 4-

hydroxynonenal: Generation and analysis of mGsta4 null mouse. Toxicol. Appl. Pharmacol 194, 296–308. [PubMed: 14761685]

Feng Z, Hu W, Tang MS, 2004 Trans-4-hydroxy-2-nonenial inhibits nucleotide excision repair human cells: A possible mechanism for lipid peroxidation-induced carcinogenesis. Proc. Natl. Acad. Sci. U. S. A 101, 8598–8602. [PubMed: 15187227]

Gates GA, Mills JH, 2005 Presbycusis. Lancet 366, 1111–1120. [PubMed: 16182900]

Han C, Ding D, Lopez MC, Manohar S, Zhang Y, Kim MJ, Park HJ, White K, Kim YH, Linser P, Tanokura M, Leeuwenburgh C, Baker HV, Salvi RJ, Someya S, 2016 Effects of long-term exercise on age-related hearing loss in mice. J. Neurosci 36, 11308–11319. [PubMed: 27807171]

Henderson CJ, Wolf CR, 2011 Knockout and transgenic mice in glutathione transferase research. Drug Metab. Rev

Herbst U, Toborek M, Kaiser S, Mattson MP, Hennig B, 1999 4-Hydroxynonenal Induces Dysfunction and Apoptosis of Cultured Endothelial Cells. J. Cell. Physiol 181, 295–303. [PubMed: 10497308]

Jenner P, 2003 Oxidative Stress in Parkinson's Disease. Ann. Neurol 53, S26–S38. [PubMed: 12666096]

Laborde E, 2010 Glutathione transferases as mediators of signaling pathways involved in cell proliferation and cell death. Cell Death Differ.

Lin CY, Wu JL, Shih TS, Tsai PJ, Sun YM, Guo YL, 2009 Glutathione S-transferase M1, T1, and P1 polymorphisms as susceptibility factors for noise-induced temporary threshold shift. Hear. Res 257, 8–15. [PubMed: 19643173]

McElwee JJ, Schuster E, Blanc E, Piper MD, Thomas JH, Patel DS, Selman C, Withers DJ, Thornton JM, Partridge L, Gems D, 2007 Evolutionary conservation of regulated longevity assurance mechanisms. Genome Biol. 8.

Müller M, Von Hünerbein K, Hoidis S, Smolders JWT, 2005 A physiological place-frequency map of the cochlea in the CBA/J mouse. Hear. Res 202, 63–73. [PubMed: 15811700]

Nebert DW, Vasiliou V, 2004 Analysis of the glutathione S-transferase (GST) gene family. Hum. Genomics 1, 460–464. [PubMed: 15607001]

Noben-Trauth K, Zheng QY, Johnson KR, 2003 Association of cadherin 23 with polygenic inheritance and genetic modification of sensorineural hearing loss. Nat. Genet 35, 21–23.

Ozmeral EJ, Eddins AC, Frisina DR, Eddins DA, 2016 Large cross-sectional study of presbycusis reveals rapid progressive decline in auditory temporal acuity. Neurobiol. Aging 43, 72–78. [PubMed: 27255816]

Park H-J, Kim M-J, Rothenberger C, Kumar A, Sampson EM, Ding D, Han C, White K, Boyd K, Manohar S, Kim Y-H, Ticsa MS, Gomez AS, Caicedo I, Bose U, Linser PJ, Miyakawa T, Tanokura M, Foster TC, Salvi R, Someya S, 2019 GSTA4 mediates reduction of cisplatin ototoxicity in female mice. Nat. Commun 10.

Park H-J, Kim M-J, Rothenberger C, Kumar A, Sampson EM, Ding D, Han C, White K, Boyd K, Manohar S, Kim Y-H, Ticsa MS, Gomez AS, Caicedo I, Bose U, Linser PJ, Miyakawa T, Tanokura M, Foster TC, Salvi R, Someya S, 2019 GSTA4 mediates reduction of cisplatin ototoxicity in female mice. Nat. Commun 10.

Rahman I, Kode A, Biswas SK, 2007 Assay for quantitative determination of glutathione and glutathione disulfide levels using enzymatic recycling method. Nat. Protoc 1, 3159–3165.

Rockwell P, Yuan H, Magnusson R, Figueiredo-Pereira ME, 2000 Proteasome inhibition in neuronal cells induces a proinflammatory response manifested by upregulation of cyclooxygenase-2, its accumulation as ubiquitin conjugates, and production of the prostaglandin PGE2. Arch. Biochem. Biophys 374, 325–333. [PubMed: 10666314]

Shearn CT, Fritz KS, Shearn AH, Saba LM, Mercer KE, Engi B, Galligan JJ, Zimniak P, Orlicky DJ, Ronis MJ, Petersen DR, 2016 Deletion of GSTA4–4 results in increased mitochondrial post-translational modification of proteins by reactive aldehydes following chronic ethanol consumption in mice. Redox Biol. 7, 68–77. [PubMed: 26654979]

Sheehan D, Meade G, Foley VM, Dowd C. a, 2001 Structure, function and evolution of glutathione transferases: implications for classification of non-mammalian members of an ancient enzyme superfamily. Biochem. Soc 360, 1–16.

Shringarpure R, Grune T, Sitte N, Davies KJA, 2000 4-Hydroxynonenal-modified amyloid-β peptide inhibits the proteasome: Possible importance in Alzheimer's disease. Cell. Mol. Life Sci 57, 1802–1809. [PubMed: 11130184]

Shuknecht HF, Watanuki K, Takahashi T, Belal AA, Kimura RS, Jones DD, Ota CY, 1974 Atrophy of the stria vascularis, a common cause for hearing loss. Laryngoscope 84, 1777–1821. [PubMed: 4138750]

Singh R, Wang Y, Schattenberg JM, Xiang Y, Czaja MJ, 2009 Chronic oxidative stress sensitizes hepatocytes to death from 4-hydroxynonenal by JNK/c-Jun overactivation. Am. J. Physiol. - Gastrointest. Liver Physiol 297, 907–917.

Srivastava S, Chandra A, Bhatnagar A, Srivastava SK, Ansari NH, 1995 Lipid peroxidation product, 4-hydroxynonenal and its conjugate with GSH are excellent substrates of bovine lens aldose reductase. Biochem Biophys Res Commun 217(3):741–746. [PubMed: 8554593]

Someya S, Xu J, Kondo K, Ding D, Salvi RJ, Yamasoba T, Rabinovitch PS, Weindruch R, Leeuwenburgh C, Tanokura M, Prolla TA, 2009 Age-related hearing loss in C57BL/6J mice is mediated by Bak-dependent mitochondrial apoptosis. Proc. Natl. Acad. Sci. U. S. A 106, 19432–19437. [PubMed: 19901338]

Someya S, Yu W, Hallows WC, Xu J, Vann JM, Leeuwenburgh C, Tanokura M, Denu JM, Prolla TA, 2010 Sirt3 mediates reduction of oxidative damage and prevention of age-related hearing loss under Caloric Restriction. Cell 143, 802–812. [PubMed: 21094524]

Van Eyken E, Van Camp G, Fransen E, Topsakal V, Hendrickx JJ, Demeester K, Van De Heyning P, Mäki-Torkko E, Hannula S, Sorri M, Jensen M, Parving A, Bille M, Baur M, Pfister M, Bonaconsa A, Mazzoli M, Orzan E, Espeso A, Stephens D, Verbruggen K, Huyghe J, Dhooge I, Huygen P, Kremer H, Cremers CWRJ, Kunst S, Manninen M, Pyykkö I, Lacava A, Steffens M, Wienker TF, Van Laer L, 2007 Contribution of the N-acetyltransferase 2 polymorphism NAT2*6A to age-related hearing impairment. J. Med. Genet 44, 570–578. [PubMed: 17513527]

Voghel G, Thorin-Trescases N, Farhat N, Mamarbachi AM, Villeneuve L, Fortier A, Perrault LP, Carrier M, Thorin E, 2008 Chronic treatment with N-acetyl-cystein delays cellular senescence in endothelial cells isolated from a subgroup of atherosclerotic patients. Mech. Ageing Dev 129, 261–270. [PubMed: 18302967]

Yamasoba T, Lin FR, Someya S, Kashio A, Sakamoto T, Kondo K, 2013 Current concepts in age-related hearing loss: Epidemiology and mechanistic pathways. Hear. Res 303, 30–38. [PubMed: 23422312]

Zheng QY, Johnson KR, Erway LC, 1999 Assessment of hearing in 80 inbred strains of mice by ABR threshold analyses. Hear. Res 130, 94–107. [PubMed: 10320101]

Zhou X, Jen PHS, Seburn KL, Frankel WN, Zheng QY, 2006 Auditory brainstem responses in 10 inbred strains of mice. Brain Res. 1091, 16–26. [PubMed: 16516865]

Zimniak P, Singhal SS, Srivastava SK, Awasthi S, Sharma R, Hayden JB, Awasthi YC, 1994 Estimation of genomic complexity, heterologous expression, and enzymatic characterization of mouse glutathione S-transferase mGSTA4–4 (GST 5.7). J. Biol. Chem 269, 992–1000. [PubMed: 7904605]

Highlights

- Loss of *Gsta4* does not increase inner ear 4-HNE levels in young or aged mice
- Loss of *Gsta4* does not promote age-related cochlear pathology in mice
- Loss of *Gsta4* does not accelerate age-related hearing loss in mice
- GSTA4 is not essential for removal of 4-HNE in mouse inner ears under normal physiological conditions

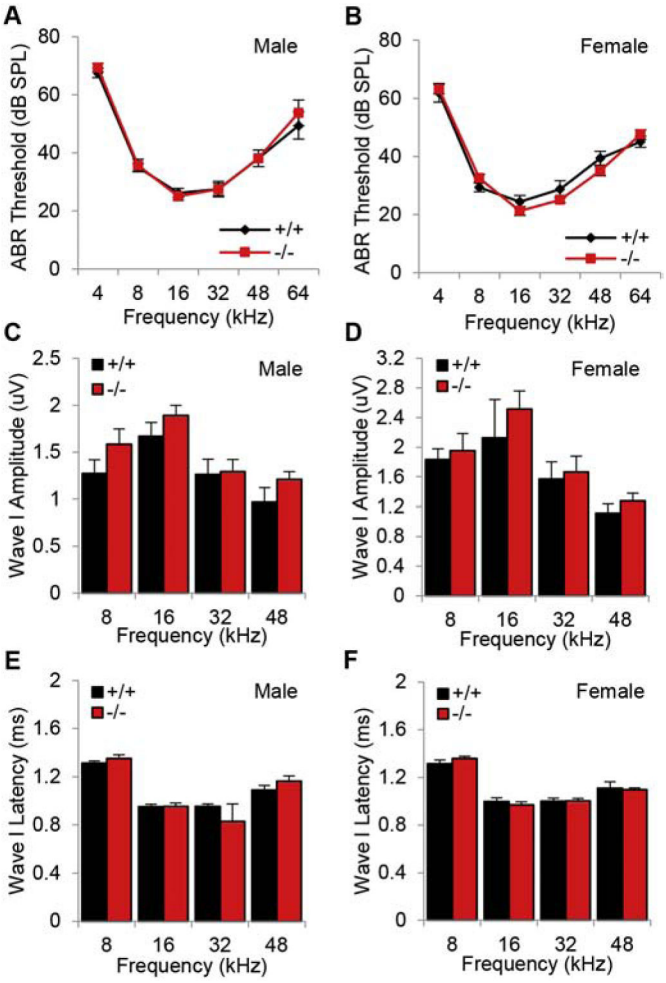

Fig 1. Assessment of ABR thresholds and wave I amplitudes and latencies in young *Gsta4*$^{+/+}$ and *Gsta4*$^{-/-}$ mice.

(A-B) ABR thresholds were measured at 4, 8, 16, 32, 48 and 64 kHz in 3–5 month-old male (A) and female (B) *Gsta4*$^{+/+}$ and *Gsta4*$^{-/-}$ mice (N=8). (C-F) ABR amplitudes (C-D) and latencies (E-F) of wave I at 90 dB were measured at 8, 16, 32, and 48 kHz in 3–5 month-old male (C,E) and female (D,F) *Gsta4*$^{+/+}$ and *Gsta4*$^{-/-}$ females (B, C) (N=8). Data are shown as means ±SEM.

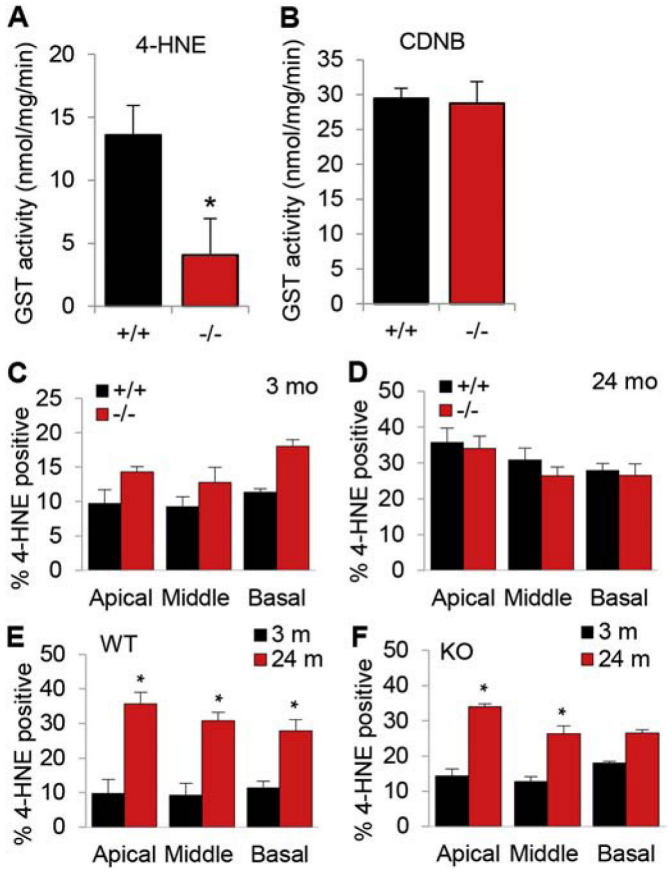

Fig 2. Assessment of GST activity in the inner ears of young *Gsta4*$^{+/+}$ and *Gsta4*$^{-/-}$ mice.

(A-B) The activities of GST toward 4-hydroxynonenal (4-HNE) (A) or CDNB (B) were measured in the cytosol of the inner ear tissues from 3–5 month-old male *Gsta4*$^{+/+}$ and *Gsta4*$^{-/-}$ mice (N=4). Data are means ±SEM. *$p < 0.05$ vs. +/+. (C-F) 4-HNE-positive SGNs were counted and quantified in the apical, middle, and basal regions of cochlear tissues from male *Gsta4*$^{+/+}$ and *Gsta4*$^{-/-}$ mice at 3–5 (C, E) and 24–25 (D, F) months of age (N=4–5). Data are means ±SEM. *$p < 0.05$ vs. 3 mo.

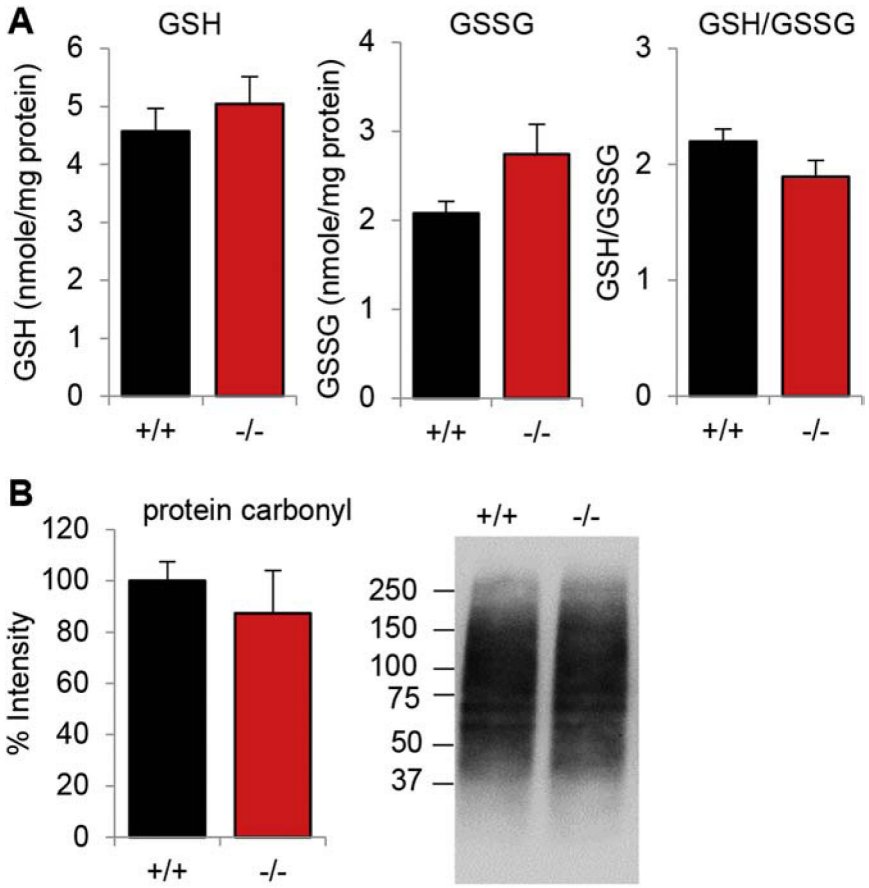

Fig 3. Assessment of glutathione redox state in the inner ears of young *Gsta4*$^{+/+}$ and *Gsta4*$^{-/-}$ mice.

(A) The levels of GSH, GSSG, and GSH/GSSG were measured in the cytosol of the inner ear tissues from 3–5 month-old *Gsta4*$^{+/+}$ and *Gsta4*$^{-/-}$ males (N=4). (B) The levels of protein carbonyl were measured in the inner ear tissues from 3–5 month-old *Gsta4*$^{+/+}$ and *Gsta4*$^{-/-}$ males (N=4–5). Data are means ±SEM.

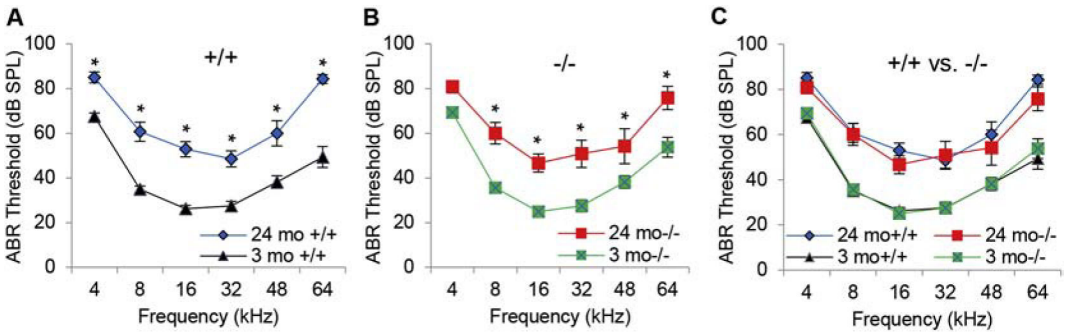

Fig 4. Assessment of ABR thresholds in young and old *Gsta4*$^{+/+-}$ and *Gsta4*$^{-/-}$ mice.

(A-C) ABR thresholds were measured at 4, 8, 16, 32, 48 and 64 kHz in 3–5 month-old male *Gsta4*$^{+/+}$ (A) and *Gsta4*$^{-/-}$ (B) mice at 3–5 (N=8) and 24–25 (N=6–7) months of age. Data are shown as means ±SEM. *$P < 0.05$ vs. 3 mo +/+ or 3 mo −/−.

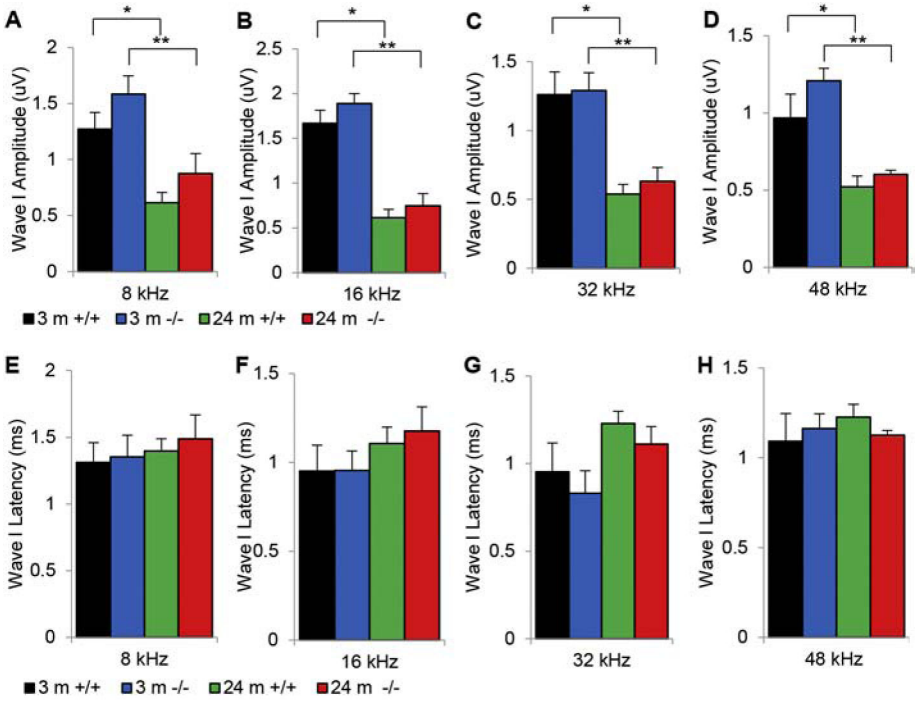

Fig 5. Assessment of ABR wave I amplitudes and latencies in young and old *Gsta4*$^{+/+-}$ and *Gsta4*$^{-/-}$ mice.

ABR amplitudes (A-D) and latencies (E-H) of wave I at 90 dB were measured at 8 (A, E), 16 (B, F), 32 (C, G), and 48 (D, H) kHz in 3–5 month-old male *Gsta4*$^{+/+}$ and *Gsta4*$^{-/-}$ mice at 3–5 (N=8) and 24–25 (N=6–7) months of age. Data are shown as means ±SEM. *$P < 0.05$ vs. 3 mo +/+ or 3 mo −/−.

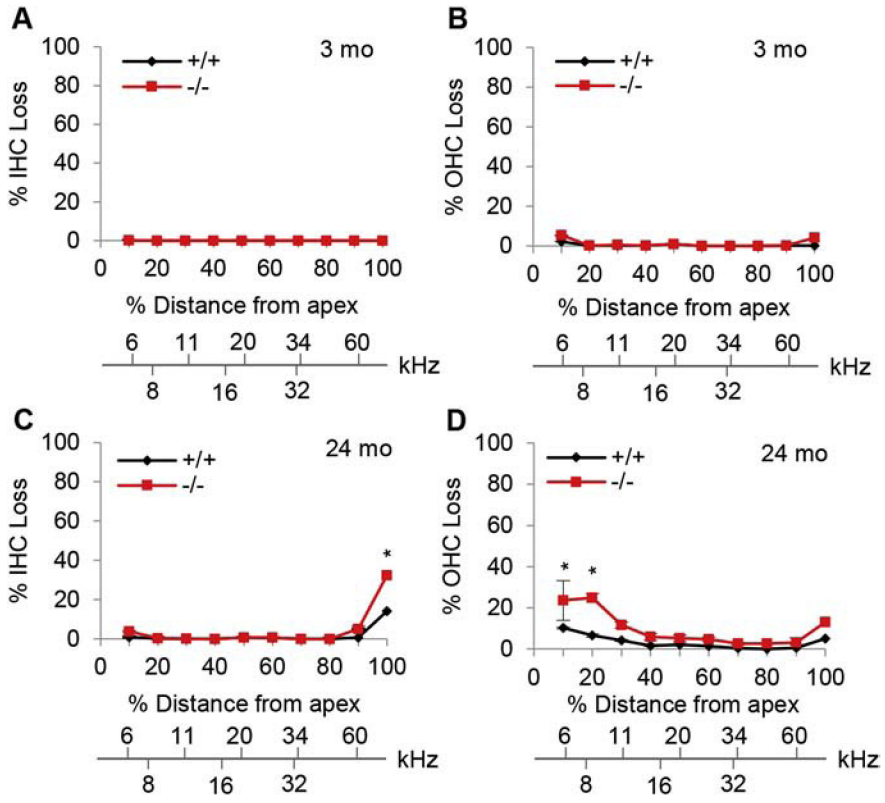

Fig 6. Cochleograms of young and old *Gsta4*$^{+/+}$ and *Gsta4*$^{-/-}$ mice.

Cochleograms were recorded and averaged in the cochlear tissues of male *Gsta4*$^{+/+}$ and *Gsta4*$^{-/-}$ mice at 3–5 (A-B) (N=4) and 24–25 month-old (C-D) (N=5–6). Graphs show percent loss of inner hair cells (IHC) (A, C) and outer hair cells (OHCs) (B, D) as function of percent distance from the apex. Lower x-axes show the frequency-place map for the mouse cochlea. Data are shown as means ±SEM. *$P < 0.05$ vs. +/+.

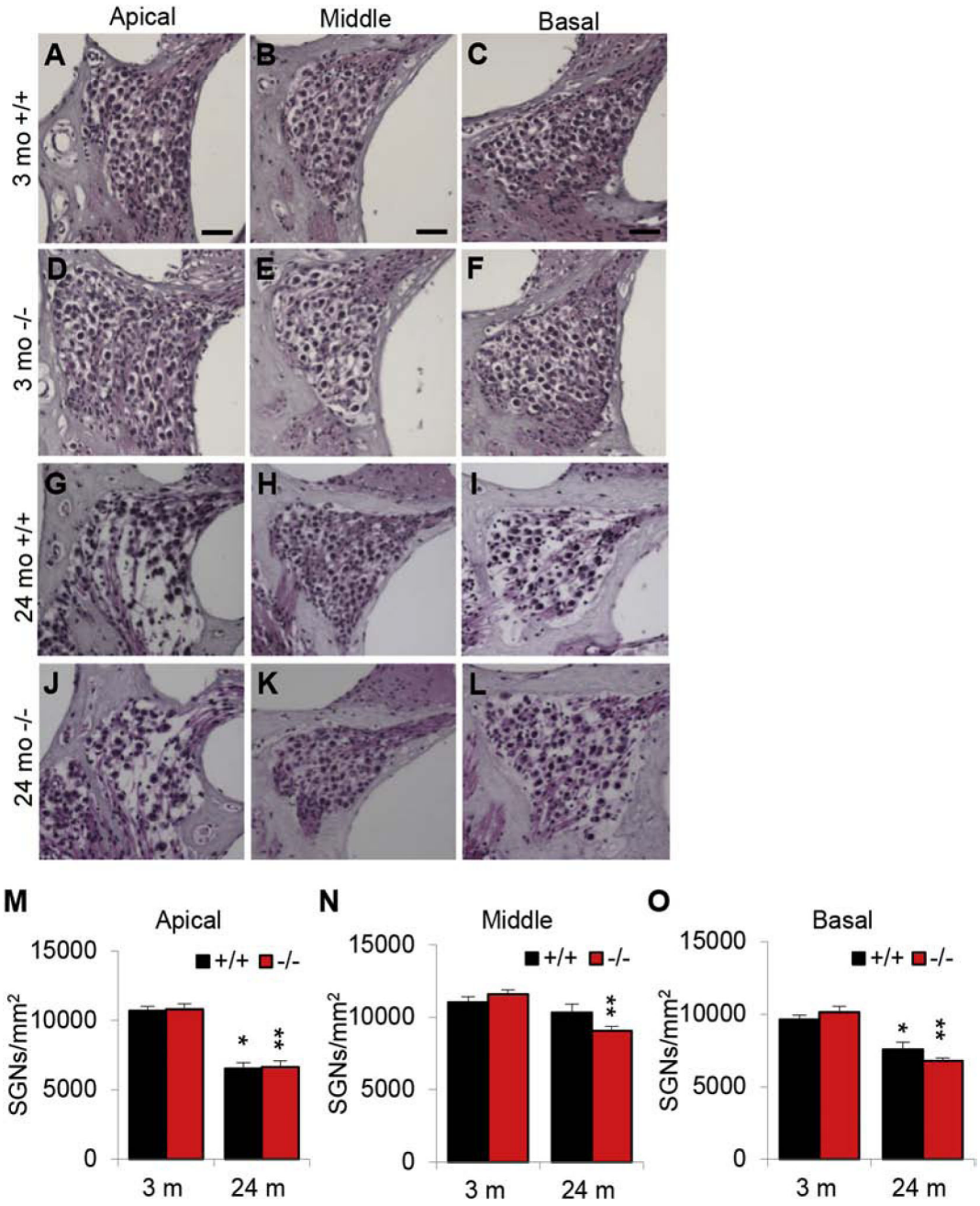

Fig 7. Assessment of cochlear SGN density in young and old *Gsta4*$^{+/+}$ and *Gsta4*$^{-/-}$ mice.

(A-L) SGN regions in the apical (A, D, G, J), middle (B, E, H, K), and basal (C, F, I, L) regions of cochlear sections from male *Gsta4*$^{+/+}$ and *Gsta4*$^{-/-}$ mice at 3–5 month-old (A-F) and 24–25 month-old (G-L). Scale bar = 20μm. SGN densities were counted and quantified in the apical (M), middle (N), and basal (O) regions of cochlear sections of male *Gsta4*$^{+/+}$ and *Gsta4*$^{-/-}$ mice at 3–5 month-old (N=3–4) and 24–25 month-old (N=5). Data are shown as means ±SEM. *$P < 0.05$ vs. 3 mo +/+. **$P < 0.05$ vs. 3 mo −/−.

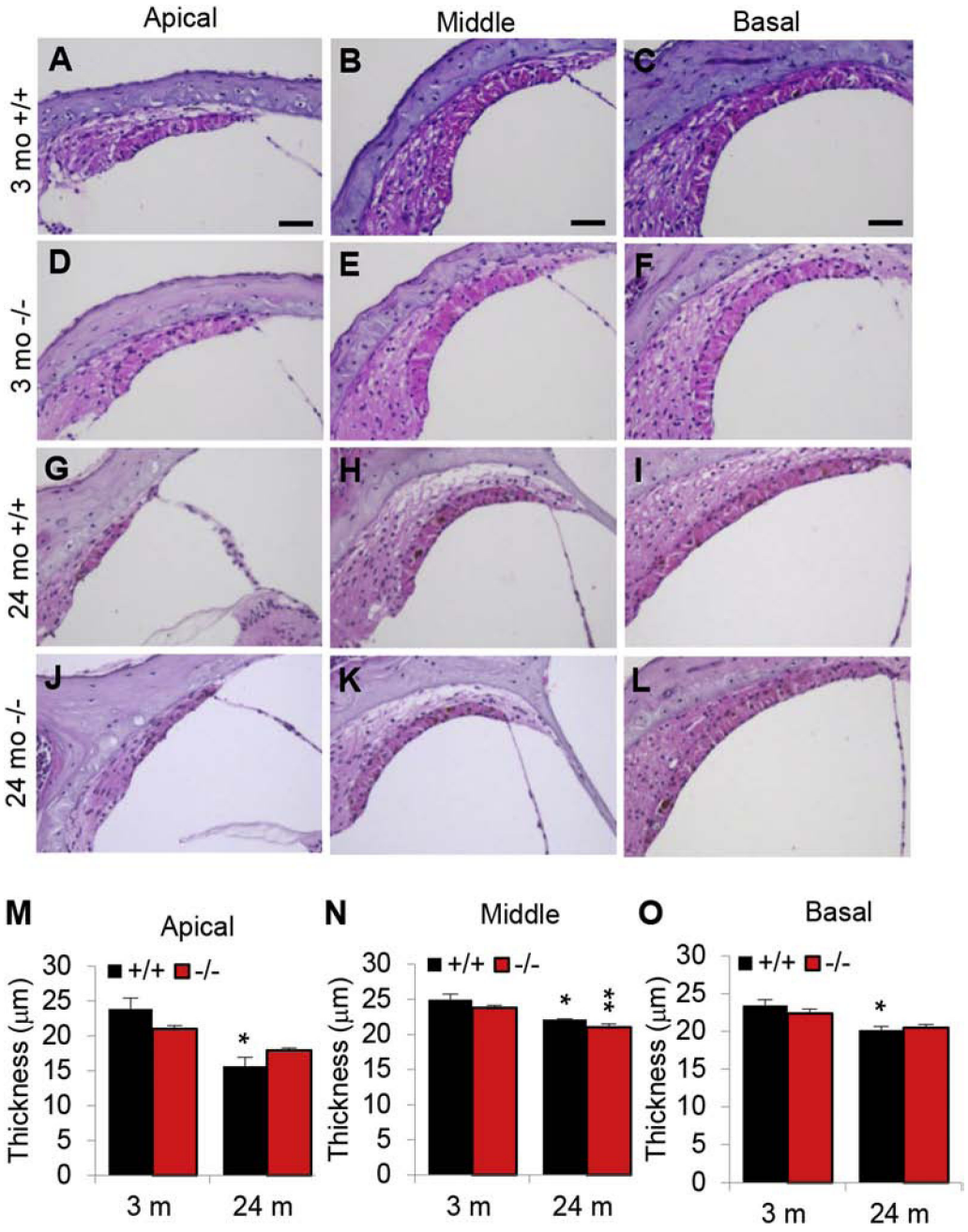

Fig 8. Assessment of SV thickness in young and old *Gsta4*$^{+/+}$ and *Gsta4*$^{-/-}$ mice.

(A-L) SV thickness in the apical (A, D, G, J), middle (B, E, H, K), and basal (C, F, I, L) regions of cochlear sections from male *Gsta4*$^{+/+}$ and *Gsta4*$^{-/-}$ mice at 3–5 month-old (A-F) and 24–25 month-old (G-L) (5). Scale bar = 20 μm. SV thickness were measured in the apical (M), middle (N), and basal (O) regions of cochlear sections of male *Gsta4*$^{+/+}$ and *Gsta4*$^{-/-}$ mice at 3–5 month-old (N=3–4) and 24–25 month-old (N=5). Data are shown as means ±SEM. *$P < 0.05$ vs. 3 mo +/+. **$P < 0.05$ vs. 3 mo −/−.